

# Performance of scintillation pixel detectors with MPPC read-out and digital signal processing

---

Makek, Mihael; Bosnar, Damir; Gačić, V.; Pavelić, Luka; Šenjug, Pavla; Žugec, Petar

Source / Izvornik: **Acta Physica Polonica B**, 2017, 48, 1721 - 1726

Journal article, Published version

Rad u časopisu, Objavljena verzija rada (izdavačev PDF)

<https://doi.org/10.5506/APhysPolB.48.1721>

Permanent link / Trajna poveznica: <https://urn.nsk.hr/urn:nbn:hr:217:090298>

Rights / Prava: [Attribution 4.0 International](#)/[Imenovanje 4.0 međunarodna](#)

Download date / Datum preuzimanja: **2024-09-18**



Repository / Repozitorij:

[Repository of the Faculty of Science - University of Zagreb](#)



## PERFORMANCE OF SCINTILLATION PIXEL DETECTORS WITH MPPC READ-OUT AND DIGITAL SIGNAL PROCESSING\*

M. MAKEK, D. BOSNAR, V. GAČIĆ, L. PAVELIĆ, P. ŠENJUG, P. ŽUGEČ

Department of Physics, Faculty of Science, University of Zagreb  
Bijenička 32, 10000 Zagreb, Croatia

*(Received August 21, 2017)*

We have assembled and tested a system of 2 detector modules containing Lutetium Fine Silicate scintillator pixels in  $4 \times 4$  matrix, read out by multi-pixel photon counter arrays with the matching element size. The amplified signals were acquired using fast digitizers and stored for offline analysis. Using two different approaches, we have determined the single crystal relative energy resolution at 511 keV to be 14% and 12%. The coincidence time resolution has been tested using the digital constant fraction triggering and the leading edge method, and the resulting resolutions are 1.6 ns and 0.5 ns, respectively.

DOI:10.5506/APhysPolB.48.1721

### 1. Introduction

The introduction of Silicon photo-multipliers (SiPM) [1] or Multi-pixel photon counters (MPPC), along with advances in scintillation materials and evolution of fast electronics, has opened numerous possibilities for improvement and minimization of detector systems used in high-energy physics, as well as in medical applications.

We have set up a detector system comprised of two modules of Lutetium Fine Silicate (LFS) [2, 3] scintillator pixels in  $4 \times 4$  configuration. The scintillation pixels are individually matched to  $4 \times 4$  MPPC arrays. All signals are read out by fast pulse digitizers and stored for offline analysis. This detector setup is used as a prototype for testing different energy and time reconstruction methods based on digital signal processing. In this paper, we report on the initial performance of the setup and we present the results of two different energy and time reconstruction schemes.

---

\* Presented at the 2<sup>nd</sup> Jagiellonian Symposium on Fundamental and Applied Subatomic Physics, Kraków, Poland, June 3–11, 2017.

## 2. Experimental setup

The system has two modules, each consisting of  $3.14 \text{ mm} \times 3.14 \text{ mm} \times 20 \text{ mm}$  LFS scintillator pixels pre-assembled by the manufacturer in a  $4 \times 4$  configuration, as illustrated in Fig. 1. The pixel pitch is 3.2 mm, each pixel is wrapped in  $\sim 0.06 \text{ mm}$  teflon tape and the module (except the side facing the MPPC) is enclosed in 1 mm aluminum housing. A  $4 \times 4$  MPPC array (Hamamatsu S13361-3050AE-04) [4] with the matching geometry is placed on top of the pixels (without optical grease) and the whole module is encapsulated in a light-proof plastic case. Each MPPC array is plugged into a passive base that is connected to a 16-channel amplifier via 12" flat cable. This new amplifier (AiT Instruments PBA16M) has been tested for the first time.

The amplifier outputs are connected to the fast pulse digitizers via coaxial cables. We use two 16-channel digitizers (CAEN mod. V1743) [5] to synchronously read the detectors. Each digitizer provides a trigger resulting from the logic OR of channels in a module that cross a desired threshold. The coincidence of the two digitizer trigger signals provides then a global trigger that causes the capture and acquisition of an event (Fig. 1).

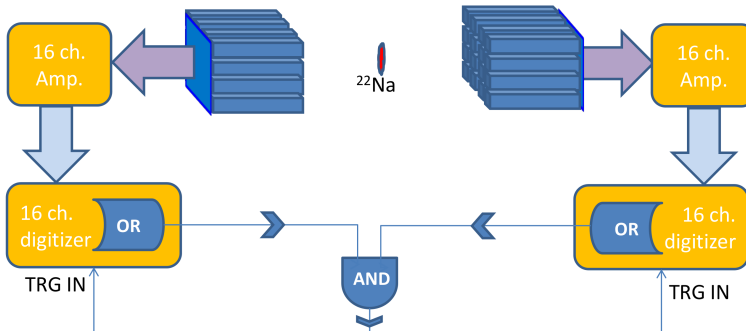


Fig. 1. The schematic view of the detector setup and trigger.

## 3. Detector system tests and performance

The system tests and calibrations were performed using two modules in coincidence setup 10 cm apart with a  $^{22}\text{Na}$  source located at the mid-point. The room temperature was  $22^\circ\text{C}$ , if not explicitly written otherwise. The digitizers were operated at 1.6 GS/s, sufficient for the signals with a typical rise-time  $t_R \sim 15 \text{ ns}$  and a decay constant of  $\tau \sim 90 \text{ ns}$ , resulting dominantly from the amplifier response.

### 3.1. Energy calibration

We apply two methods to extract the raw energy information from the digitized signals: the first measures the amplitude of the signal, and the second uses signal integration. An example of a raw energy spectrum of  $^{22}\text{Na}$  source is shown in Fig. 2 (left).

Each MPPC has a finite number ( $M = 3584$ ) of micro cells, hence as the number of scintillation photons ( $N_{\text{ph}}$ ) grows, the probability to hit already fired cells increases and the signal linearity with the energy deposition is no longer maintained [6]:

$$N_{\text{fired}} = M \left( 1 - e^{-\frac{\text{PDE } N_{\text{ph}}}{M}} \right), \quad (1)$$

where PDE is the photon detection efficiency and  $N_{\text{fired}}$  is the number of fired micro cells. To re-establish the linear relation, we apply the correction according to

$$I^* = -I \ln(1 - n) / n, \quad (2)$$

where  $I$  and  $I^*$  are the raw and the corrected integral of the signal, respectively,  $n$  is the fraction of fired micro cells, calculated for each signal according to  $n = A/Ma$ , where  $A$  is the amplitude of the signal, and  $a$  is one-photo-electron amplitude, pre-determined depending on bias voltage and temperature using digital oscilloscope. Typically, we observe  $\sim 400$  fired cells at 511 keV. The corrected spectrum of each crystal pixel is calibrated using the annihilation peak:  $E = k I^* + l$ , with  $l = 0$ , since the offsets are stable at zero. The procedure is verified by inspecting the combined spectrum of  $^{176}\text{Lu}$  (intrinsic to LFS) and  $^{22}\text{Na}$ , Fig. 2 (right), obtained in a special trigger configuration without the coincidence condition.

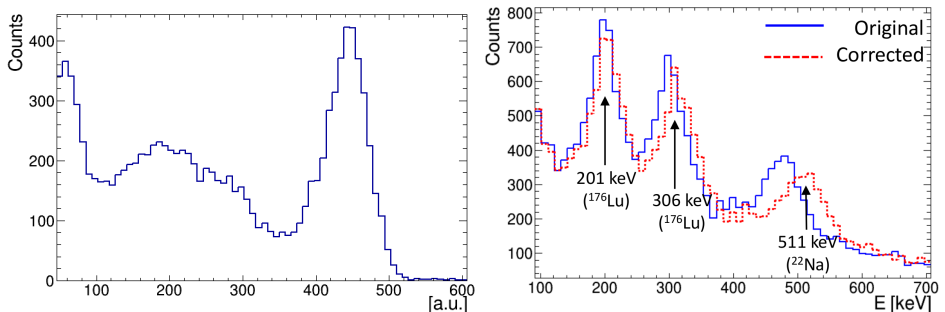


Fig. 2. Left: a single crystal raw spectrum from  $^{22}\text{Na}$  source obtained by signal integration. Right: the calibrated spectrum of  $^{176}\text{Lu}$  and  $^{22}\text{Na}$  before (solid) and after (dashed) the non-linearity correction.

### 3.2. Energy resolution

We have compared the relative energy resolution of single crystals at 511 keV,  $\Delta E/E$ , using the amplitude and the integral methods at different bias voltages,  $U$ , as seen in Fig. 3. The integral method is consistently superior, reaching  $\Delta E/E \sim 12\%$  at  $U = 54$  V, which corresponds to an overvoltage of 2 V above the break down voltage,  $V_{br}$ , while the resolution via amplitude method reaches  $\Delta E/E \sim 14\%$  at the same voltage. The improvement of the resolution with increasing bias voltage is clearly visible. This is expected owing to the rise of the PDE and, consequently, the number of fired cells for a given energy deposition. Although the observed trend indicates further improvement of the resolution at higher voltages, the measurements at  $U > 54$  V were limited by very high signals causing amplifier saturation.

We have observed a non-negligible amount of light-sharing between the adjacent crystals: by selecting a photo-peak in a (leading) pixel, we observe signals of  $\sim 5\%$  of that amplitude in each of the adjacent four neighbors. Thus, the central pixel contains  $\sim 80\%$  of the total light produced by a particle. This degrades the resolution by a factor  $\sim 1.1$ . Clearly, a more efficient reflector is needed to avoid the light-sharing.

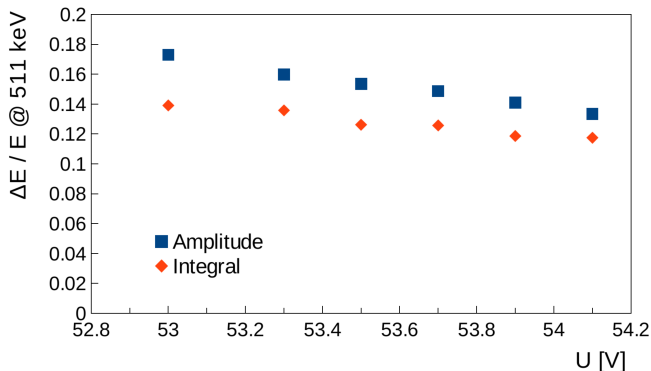


Fig. 3. Relative energy resolution at 511 keV *versus* bias voltage for the amplitude and the integral methods (see the text). The breakdown voltage is  $V_{br} = 52.0$  V.

Concerning the change of the  $\Delta E/E$  with temperature, we have not observed any significant dependence in the 18–23 °C range.

### 3.3. Coincidence time resolution

Two different approaches for the reconstruction of time difference between the coincident signals have been used. The first one is the digital constant fraction triggering. This is graphically depicted in Fig. 4 (left).

Here, we first determine the maximum of the signal by fitting the second order polynomial around the sample with the maximum amplitude,  $A$ . Then a straight line is the fit on the rising edge of the signal, and the time,  $t$ , is determined from this fit as the  $x$ -coordinate at  $y = fA$ , where  $f$  is the desired fraction of the signal maximum. An example of  $\Delta t$  distribution for  $f = 0.15$  is shown in Fig. 4 (right). For the signals belonging to the annihilation peak, the coincidence time resolution (CTR) is  $\Delta T = 1.6$  ns (FWHM).

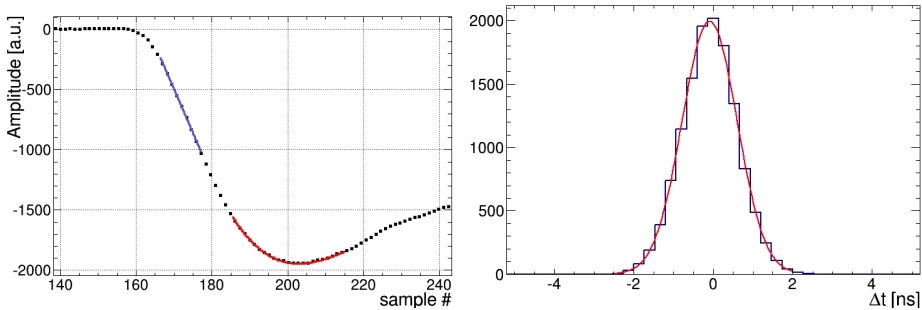


Fig. 4. Time determination using digital constant fraction method. Left: an example of the time determination (see the text for details). Right: coincidence time distribution with  $\Delta T = 1.6$  ns.

The other approach uses time pick off at the leading edge of the signal. First, we find the sample,  $s$ , on the leading edge closest to a given threshold. A straight line is then fit through five samples in the range from  $s - 2$  to  $s + 2$ . The time,  $t$ , is determined from the fit as the  $x$ -coordinate at  $y = \text{threshold}$ . This is graphically depicted in Fig. 5 (left). Additionally, to reduce the fluctuations, we derive the time difference at three different

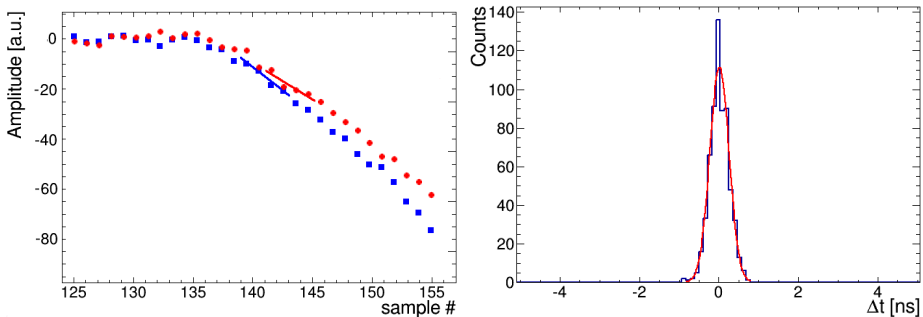


Fig. 5. Time determination using digital leading edge method. Left: an example of the time determination for a threshold of  $-20$ , showing both coincident signals. Only one threshold fit per signal is depicted for clarity. The full method uses 3 thresholds (see the text for details). Right: coincidence time distribution with  $\Delta T = 0.5$  ns.

thresholds and calculate the average:  $\Delta t = \frac{1}{3}(\Delta t(1) + \Delta t(2) + \Delta t(3))$ . For the threshold  $(1, 2, 3) = -20, -25, -30$ , we obtain  $\Delta T = 0.5$  ns (FWHM), Fig. 5 (right), again with the condition that the signals belong to the annihilation peak. The previous work has reported the CTR of the LFS  $< 200$  ps [7, 8], using, however, shorter crystals (15 mm) and much higher over-voltage (up to +5 V). The preliminary investigation using our setup indicates prospects for significant improvement with lower triggering thresholds and higher over-voltages.

#### 4. Summary

We have assembled and tested a system of 2 detector modules, each consisting of 16 LFS scintillator crystals in  $4 \times 4$  matrix read out with the matching MPPC arrays. All 32 channels are individually amplified with new 16 channel amplifiers, and fed into fast waveform digitizers at the sampling rate of 1.6 GS/s. Two different methods for the reconstruction of energy and time response have been evaluated. We have obtained the  $\Delta E/E$  at 511 keV of 14% by measuring the signal amplitude and 12% by integrating the signal. For the coincidence time resolution, we have obtained  $\Delta T = 1.6$  ns (FWHM) for the digital constant fraction method and  $\Delta T = 0.5$  ns (FWHM) for the leading edge method.

The work presented in this contribution has been supported by the Croatian Science Foundation project No. 1680 and by the Croatian Agency for Small and Medium Enterprises, Innovations and Investments (HAMAG-BICRO), Proof-of-Concept Programme, project PoC6\_1\_211.

#### REFERENCES

- [1] V. Golovin, V. Saveliev, *Nucl. Instrum. Methods Phys. Res. A* **518**, 560 (2004).
- [2] A.I. Zagumennyi, Y.D. Zavartsev, S.A. Kutovoi, US Patent 7132060, 2006, <https://www.google.ch/patents/US7132060>
- [3] LFS White Paper, <http://www.zecotek.com/media/LFSWhitePaper.pdf>
- [4] MPPC Array S13361-3050AE-04, <https://www.hamamatsu.com>
- [5] 16-Channel 12bit 3.2 GS/s Digitizer — V1743, <http://www.caen.it>
- [6] Introduction to SiPM, Technical note, <http://www.sens1.com>
- [7] M. Yamazaki, T. Takeshita, Y. Hasegawa, *JINST* **7**, P10014 (2012).
- [8] K. Doroud *et al.*, *Nucl. Instrum. Methods Phys. Res. A* **793**, 57 (2015).